

# Characterisation of Photomultipliers for LHCb Upgrade II

Author: Alejandro Rodríguez Alvarez

Facultat de Física, Universitat de Barcelona, Diagonal 645, 08028 Barcelona, Spain.

Advisor: Ricardo Vazquez Gomez

**Abstract:** With the advent of LHCb Upgrade II new technologies in detection are required to keep up with the increased luminosity. One of the technologies developed are new Photomultiplier Tubes (PMTs), capable of amplifying the received signal. These new PMTs must have a time resolution below 50 ps. In this end of degree project I characterised two PMTs manufactured by Hamamatsu, the R11187 and the R14755U-100. The characterisation consisted in measurements of time resolution in both devices and a gain measurement in the first one. The values obtained for the time resolution are below the threshold of 50 ps and the gain ( $G = 7 \times 10^5$ ) is compatible with the requirements for the detector.

## I. INTRODUCTION

The LHCb experiment is one of the four large experiments at CERN's Large Hadron Collider, alongside with CMS, ATLAS and ALICE. The main goal of LHCb is to study the CP-symmetry violation through the observation of decays in particles containing  $b$  and  $\bar{b}$  quarks such as B mesons (bound states of *bottom* quarks and light *anti-quarks*).

The results obtained so far at LHCb have supposed an unprecedented step forward in heavy flavour-physics. Under the new High Luminosity (HL-LHC) regime in which LHC will be running after Long Shutdown 3 (LS3) an upgrade for LHCb is strongly required [1]. Thus, the LHCb Upgrade II (which will start its operational period after LS4) is aimed towards making use of all the capabilities available during that period.

### A. LHCb Upgrade II

The LHCb Upgrade II will be installed in LS4, starting its operational period during Run 5, scheduled to start in 2035 as a consequence of delays due to the COVID-19 Pandemic. After the upgrade, the experiment is expected to run under instantaneous luminosities of  $2 \times 10^{34} \text{cm}^{-2} \text{s}^{-1}$  and the LHCb experiment will be able to accumulate data corresponding to  $300 \text{fb}^{-1}$ . At LHCb Runs 1 and 2, the collisions took place at instantaneous luminosities of around  $4 \times 10^{32} \text{cm}^{-2} \text{s}^{-1}$  and integrated luminosity of  $8 \text{fb}^{-1}$  was collected. After Upgrade I the peak luminosity will be about  $2 \times 10^{33} \text{cm}^{-2} \text{s}^{-1}$  and the integrated value is expected to be  $50 \text{fb}^{-1}$  [2].

Therefore, if we compare the expected luminosities after Upgrade II, they will be about 50 times larger than those in the first runs of LHC and an order of magnitude bigger than in the prior upgrade. The differences could grow even larger once there is a better understanding of the response to radiation damage as the collaboration could increase the luminosities without damaging the equipment. With the increased capabilities of Upgrade II, LHCb aims to have more precise measurements

of B-hadron decays.

There will be an offset between the beginning of the operational period of HL-LHC (starting in Run 4) and LHCb Upgrade II (starting in Run 5). This is in order to allow Upgrade I to complete its programme and to supply R&D strategies with sufficient time to develop new technologies, essential for the upgrade. Amongst which we can find the recent new SPACAL (Spaghetti Calorimeter) prototype with scintillating crystal fibres recently tested [3]. This kind of projects aim to develop new detector structures which have a time resolution below 50 ps [1].

This end of degree paper aims to be part of one of these R&D programmes. In collaboration with ICCUB I have carried out the characterisation of two Photomultiplier Tubes (PMTs) and studied its viability of implementation for the new Electromagnetic Calorimeter in LHCb Upgrade II.

## II. CHARACTERISATION OF PHOTOMULTIPLIER TUBES

### A. Photomultiplier tubes

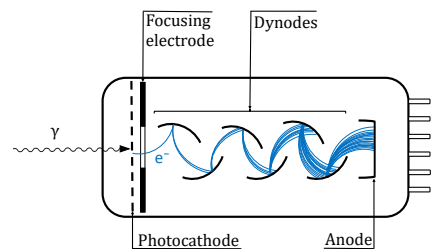


Figure 1: Scheme of the functioning of a PMT.

A Photomultiplier tube is a device which drastically amplifies the current produced by incident light. As it can be seen in Figure 1, its functioning is relatively simple: Light enters the device by a window where it encounters a photocathode, a material which then emits elec-

trons into the vacuum due to photoelectric effect. The emitted electrons are then accelerated by an electric field (provided by a voltage applied to the device) then reach a dynode which multiplies them by means of secondary emission. This process is repeated through various stages until the multiplied secondary electrons emitted by the last dynode are collected by the anode.

It is important to point out the fact that not every photon which reaches the photocathode of the PMT will produce an electron by means of photoelectric effect. This process is ruled by a probability distribution function. Therefore, we can express the ratio between the output of electrons and the incident photons as the Quantum Efficiency (QE) [4]

## B. Experimental set-up

The experimental set up for the characterisation of the Photomultiplier tubes (PMTs), as we can see in Figure 2, consisted in a red laser source which pulsed light through an optical fibre wire to a collimator that illuminated the PMT. In the series of experiments carried out I used two different photomultiplier tubes:

- The Hamamatsu R11187, an 8 dynode stages head-on photomultiplier with a bialkali photocathode [5].
- The Hamamatsu R14755U-100, a 6 dynode stages metal package photomultiplier with a super bialkali photocathode [6].

The PMTs had a high voltage input which provided voltages between 450 V and 700 V in our measurements. As an output, the device studied was connected to an oscilloscope. For the single photoelectron measurements, we added a 1.2 k $\Omega$  transimpedance amplifier between the PMT and the oscilloscope in pursuance of having less relative signal noise. The amplifier fed a differential voltage to the oscilloscope.

In addition to the PMT, the oscilloscope was connected to the laser source (either directly or through the amplifier), which sent the signal of the emitted light pulse to be used as the trigger for the measurements. Finally, the oscilloscope was connected to a computer and through a *Python* program I developed, I was able to control it and visualise the output data. The in-depth functioning of the program will be discussed in the following sections, but mainly it received a series of voltage values provided by the oscilloscope, each value equally spaced by a time determined by the sampling frequency of the device. Each of these series provided one value for the time delay between the laser trigger signal and the PMT response. A thousand series were taken in order to have a distribution of the time delay. I also explored the possibility of making more sub-measurements with regard to obtaining a more reliable statistical behaviour. However, I saw that while there were no significant changes in the results obtained, increasing the sub-measurements

produced a notable increment in the time spent both collecting the measurement data and processing it.

In addition to the foregoing, as the PMT had to be run under low light conditions to avoid burning it (they are very sensitive devices designed to receive just a few photons at a time in the photocathode), the laser collimator and the PMT were enclosed in a black box, sealed as good as possible to avoid getting undesired signal noise.

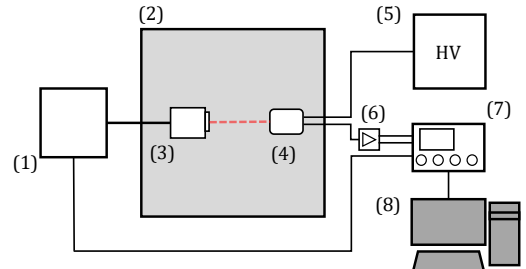


Figure 2: Diagram of the experimental set-up used for the characterisation of PMTs. (1) Laser light source, (2) Black box, (3) Laser collimator, (4) PMT, (5) High Voltage source, (6) Transimpedance amplifier, (7) Oscilloscope, (8) Computer

## C. Measurement process

To characterise the gain and time resolution of the different PMTs we studied the shape of the signal obtained in many measurements under the same conditions of voltage and laser intensity. Taking into account how does the PMT work, it is easy to understand the shape of the output signal (Figure 3): a fast sudden increase in voltages at the beginning of the waveform and a slower decrease with even a small queue at the end which is due to the fact that there are still secondary electrons reaching the anode once the bulk of them has arrived.

The main measurement to make was the time between the laser trigger signal started and the PMT gave a response (the green arrow in Figure 3). These time values were then stored so we could find the expected value ( $\mu_t$ ) and its standard deviation ( $\sigma_t$ ). This standard deviation was the time resolution for our device. It is also worth mentioning that plotting histograms of the response time of the PMT we expected to find a Gaussian distribution because notwithstanding the fact that the number of photoelectrons created in the photomultiplier tube follows a Poisson distribution [7], for a large enough number of photons entering the device, the distribution becomes Gaussian.

### 1. Time resolution measurements

When it comes to doing the measurement of the time, I first had to set a threshold which would determine when

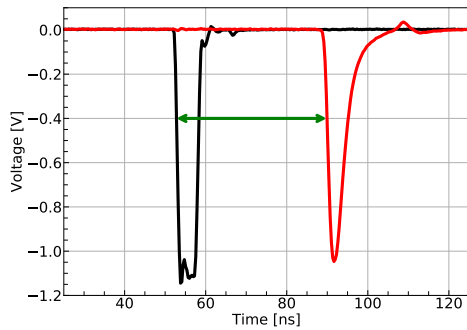


Figure 3: Typical signal obtained in a PMT response signal. In black, the laser pulse that serves as trigger for the measurement. In red, the PMT output signal and in green an arrow representing the time we measure between the emission of the trigger pulse until the beginning of the output signal.

did a signal arrive allowing us to differentiate it from the noise. To set the threshold, there were many factors to consider. Firstly, the threshold was a variable value, which corresponded to a percentage of the height of the peak (amplitude). To set said percentage, the program performed the time resolution measurement in a range of amplitude percentages between 10% and 90%. This way, I could find the optimal percentage for every measurement depending on the voltage and the laser intensity. I used a variable threshold value because when using a constant threshold, signal suffers from time walk effects [8], which is the fact that for lower amplitude peaks, we would obtain a delayed response compared to taller signals, as seen in Figure 4.

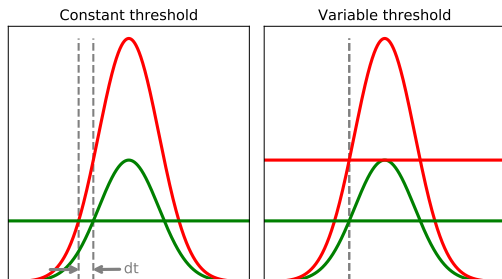


Figure 4: Representation of time walk effects. To the left we can see a delay in time as signals get smaller if we have set a constant threshold. To the right, the delay disappears if we use a variable threshold.

Once we had decided how and where to set the threshold, the next step was making the program find where did the signal cross it. To develop this task, the program scanned the data and returned the value in which the signal went over (below in this case) the threshold as well as the previous value.

Since the oscilloscope had a limited data collecting frequency (3.2 GHz) every voltage measurement was sepa-

rated by 312.5 ps. This created a problem because regardless of how close to one of the ends of the interval the threshold line was, the program would always return the same time value. To address this issue an interpolation in the interval in which the signal crossed the threshold was implemented to the program. I also tried using a linear fit taking a set of data points before and after the threshold. However, this method gave some problems with “small” signals.

## 2. Gain measurements

On the other hand, to measure the gain of the devices, we explored two different methodologies, both from the starting point that the gain is defined as the ratio between the anode current and the photocathode current [9], also defined using the following formula:

$$Q = N_{p.e.} \times G \times e \quad (1)$$

where  $Q$  is the charge in the anode,  $N_{p.e.}$  is the number of photoelectrons in the cathode,  $G$  is the gain and  $e$  is the electron charge.

The first method is using a statistic approach to the problem. We can calculate the charge output in the anode using the voltage values from our data array (bearing in mind we have to subtract the charge generated by the background noise in the signal) as it is done in equation (2) [10].

$$Q = \int_0^{t_f} \frac{V}{R} dt \quad (2)$$

To find the number of photoelectrons, we use equation (3), where  $\mu$  and  $\sigma$  are the expected value and the standard deviation of the charge of the signal peak or the charge of the pedestal (the part of the signal where there is no PMT response, only background noise).

$$N_{p.e.} = \frac{(\mu_{signal} - \mu_{pedestal})^2}{\sigma_{signal}^2 - \sigma_{pedestal}^2} \quad (3)$$

We use this approximation regarding the probability that a certain number of secondary electrons are generated in every dynode stage is related to the output charge [10].

The alternative method was making what is known as “Single photoelectron events” (SPE) measurements, which consist in dimming the laser light until the point in which just one photon enters the PMT. Obviously, this is nearly impossible, so in fact the number of photons entering the device is around 10 but only the 10% of the light will generate PMT response [7]. This way we obtain a charge histogram which follows a Poisson

distribution centred around the charge output. Then, integrating the charge output like in equation (2) and supposing we have one photoelectron in the photocathode, equation (1) gives us the gain instantly. While this method is not perfect, as one could argue that we can't assure that the gain for one photoelectron will be the same for a higher number of them, it is the most accepted method to characterise gain, so it is the one we used for our characterisation.

### 3. Single Photoelectron measurements

To carry out the single photoelectron event (SPE) measurements we placed a series of optical attenuators before the PMT to dim the laser light. My PMT choice was the R11187, as according to the manufacturer it had a slightly higher gain than the R14755U-100 (making it more likely to detect a single photoelectron). The process of obtaining the measurements consisted in using the program to capture a data array as explained in section II.B, with the nuance that as the amplifier gave a differential output voltage, the program had to add both parts of the voltage to get the real signal of the PMT. With our array of voltages, I calculated the charge in every sub-measurement using equation (2) and plotted histograms to later fit a Gaussian curve to them. This way we could find the output charge in the anode and with equation (1) determine the gain of the PMT. Although the number of electrons produced follows a Poisson distribution, we can use a Gaussian fit provided the large number of events registered.

## III. RESULTS

Time resolution has a strong dependence on the voltage applied to the PMT. Therefore, we performed measurements for both PMTs at a very high voltage (700 V) and at a voltage similar to the one under which they could be running during its lifetime at the Electromagnetic Calorimeter (450 V). To compute the gain, on the other hand due to set-up limitations I could only make measurements at 800 V as at lower voltages the single photoelectron peak was completely indistinguishable.

### A. Time resolution

We can see in Figure 5 that there is a small peak before the main Gaussian peak, this could be due to photoelectrons extracted directly from the first dynode instead of the photocathode [7] regarding the fact that when using a collimator before the PMT, the secondary peak disappears (as light is focused more punctually on the photocathode). In addition to that, we can see that this phenomenon does not happen for the other PMT (Figure

6) as the possibility of reaching directly the first dynode depends on the construction of the device.

If we examine the main peak, it fits easily into a Gaussian distribution. For both the examined photomultiplier tubes the time resolution results are promising, as they are way below the maximum  $\sigma_t = 50$  ps pursued. In Table I we can see the results for both PMTs at the studied voltages and laser intensities.

Table I: Results for time resolution for both PMTs

PMT	Voltage [V]	Laser Intensity [A.U.]	$\sigma_t$ [ps]
R11187	450	2.8	34.039
		3.5	24.777
	700	2.8	13.740
		3.5	14.605
R14755U-100	450	2.8	19.689
		3.5	12.754
	700	2.8	15.632
		3.5	10.950

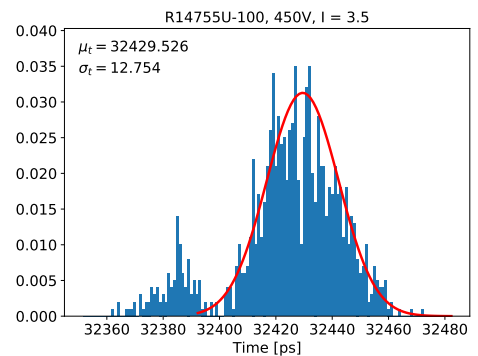


Figure 5: Normalised time histogram for the Hamamatsu R14755U-100 under a voltage of 450 V and with a light intensity of 3.5.

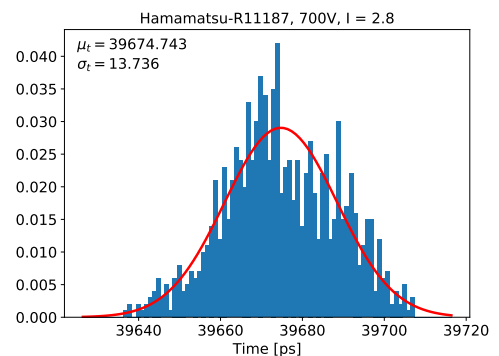


Figure 6: Normalised time histogram for the Hamamatsu R11187 under a voltage of 700 V and with a light intensity of 2.8.

## B. Gain measurements

For the gain measurements we obtain a charge histogram like the one in Figure 7, where, on the left, the bin at zero corresponds to every event registered in which no electron was produced in the photocathode, and the rest of the distribution is associated to the PMT signal. Just as we expected the zero-photoelectron peak is about a hundred times higher than the single photoelectron. If we now fit a Gaussian distribution to the single photoelectron part (Figure 7 right), we can find the value of the output charge in the anode as the expected value of the distribution ( $\mu = 0.118$  pC). Using equation (1), we obtain a gain of  $7 \times 10^5$ .

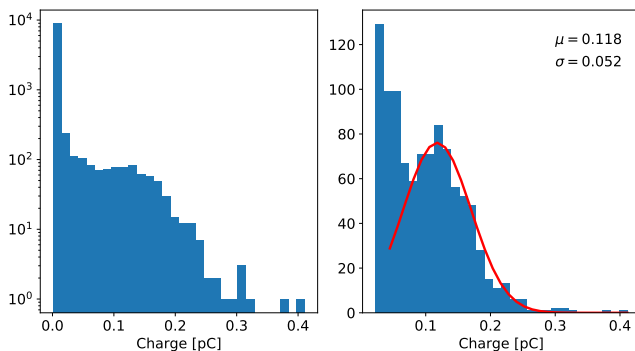


Figure 7: SPE measurements for the Hamamatsu R11187 under a voltage of 800 V and with a light intensity of 2.05. To the left the complete histogram, to the right the histogram without the bins containing the bulk of the peak when no signal is produced in the device.

## IV. CONCLUSIONS

When it comes to the time resolution, both PMTs seem to reach the requirements. With a time resolution mostly

below the 30 ps, there would still be margin to reduce the applied voltage idling around in the vicinity of the pursued 50 ps.

Despite the foregoing, there are many other factors that could make the PMTs unsuitable for their installation at the new LHCb Electromagnetic Calorimeter. For instance, the transit time (TT) that is the time delayed since a light pulse arrives at the photocathode and until the appearance of the signal pulse [4] and its non-uniformity (transit time spread or TTS). The TT could have great influence in the time resolution of the devices. In addition to that, not only time resolution is important, but also other aspects like pricing (as thousands of them are required for the Calorimeter), radiation hardness (as they will be exposed to large amounts of ionising radiation originated in particle decays) or the lack of uniformity on the photocathode response depending on both the position and the incidence angle.

When it comes to the gain of the Hamamatsu R11187, the results are compatible with those specified by the manufacturer and could be compatible with the necessities of the detector.

Although I could not characterise some of the parameters of the PMTs, this deeper analysis is being carried out or will be carried out in the near future and with the data we have to this point, both devices look like strong candidates for different regions of the detector.

## Acknowledgments

I would like to thank my advisor Ricardo Vazquez and Eduardo Picatoste for guiding me through this project as well as ICCUB for hosting me during the experimental process. I would also like to thank my family and friends for their great support and ease every time I needed it.

- 
- [1] LHCb collaboration. (2018). *Physics case for an LHCb Upgrade II. Opportunities in flavour physics, and beyond, in the HL-LHC era*. CERN-LHCC-2018-027 LHCb-PUB-2018-009.
  - [2] LHCb collaboration. (2017). *Expression of Interest for a Phase-II LHCb Upgrade: Opportunities in flavour physics, and beyond, in the HL-LHC era.*, CERN-LHCC-2017-003.
  - [3] An, L., et al. (2022). *Performance of a spaghetti calorimeter prototype with tungsten absorber and garnet crystal fibres*. <http://arxiv.org/abs/2205.02500>
  - [4] Polyakov, S. V. (2007) *PHOTOMULTIPLIER TUBES. Basics and Applications*, (Hamamatsu, 3rd. ed.).
  - [5] Hamamatsu. (2009). *Head-on Photomultiplier Tube R11187 Series*. Datasheet.
  - [6] Hamamatsu. (2021). *Metal Package Photomultiplier Tube R14755U Series*. Datasheet.
  - [7] Kaether, F., Langbrandtner, C. (2012). *Transit time and charge correlations of single photoelectron events in R7081 photomultiplier tubes*. Journal of Inst, 7(09), P09002–P09002.
  - [8] Du, J., et al. (2017). *A Time-Walk Correction Method for PET Detectors Based on Leading Edge Discriminators*. IEEE Transactions on Radiation and Plasma Medical Sciences, 1(5), 385–390.
  - [9] Photonis. *Photomultiplier tube basics*. <https://psec.uchicago.edu/library/photomultipliers>
  - [10] Montarou, G., et al. (1997). *Characterization of the Hamamatsu 10-stages R5900 photomultipliers at Clermont for the TILE calorimeter*.